Tin-Coupled Star-Shaped Block Copolymer of Styrene and Butadiene (I) Synthesis and Characterization

Huadong Feng, Xingying Zhang, Suhe Zhao

Key Laboratory on Preparation and Processing of Novel Polymer Materials, Beijing University of Chemical Technology, Beijing 100029, China

Received 31 January 2008; accepted 30 April 2008
DOI 10.1002/app.28622
Published online 18 June 2008 in Wiley InterScience (www.interscience.wiley.com).

ABSTRACT: A new kind of star-shaped block copolymer: tin-coupled polybutadiene-*b*-ploy(styrene-butadiene) ((SB-B)$_4$Sn) was synthesized by two-stage anionic polymerization technology. A novel multifunctional organo-lithium was used as initiator, and two different types of copolymers were formed, namely, *S*-PB-PSB and *S*-PB-PSB-PS, depending on the styrene content in loading solution (St%). In copolymerization, the homo-polybutadiene block was formed in the first reaction stage, and the residual blocks were formed in the second stage with the presence of tetrahydrofuran (THF). *S*-PB-PSB was synthesized when the St% was lower than 34.9%, otherwise *S*-PB-PSB-PS was generated. Nuclear magnetic resonance (NMR) results showed that the amount of vinyl based upon the butadiene content within poly(butadiene-styrene) blocks decreased dramatically as the St% was increased. Dynamic mechanical thermal analyzer (DMTA) spectra showed broadened loss peak as the St% was increased. Transmission electron microscopy (TEM) was employed to characterize the copolymer morphology, and the results showed different phase-separated morphologies as St% increased. Mechanical property testing results indicated that these two copolymers met the requirements of high performance tire tread. © 2008 Wiley Periodicals, Inc. J Appl Polym Sci 110: 228–236, 2008

Key words: synthesis; block copolymers; star polymers; mechanical properties; phase separation

INTRODUCTION

Wet skid resistance, rolling resistance, and wear characteristics are important properties to rubber materials used as tire tread.[1] Rubbers with a high rebound (like polybutadiene rubber) have traditionally been utilized in tire tread for energy-saving because of their low rolling resistance. On the other hand, rubbers which undergo a large energy loss have generally been utilized in tire tread to improve the safety because of their high wet skid resistance and good traction characteristics.[2]

In recent years, high performance tire tread requires a good overall balance of properties, especially between high wet skid resistance and low rolling resistance. However, it has traditionally been very difficult to improve a tire's rolling resistance without sacrificing its wet skid resistance and traction characteristics.[1,3] To meet the high performance requirement, generally, mixtures of various types of synthetic and natural rubbers are normally utilized in tire treads.[4] However, such blends are not satisfactory for all purposes.[5] Thus, a lot of studies have been focused on rubber materials with novel architectures, which are prepared by macromolecule design.

According to the structure–property relationship of polymer, both rolling resistance and wet skid resistance are related to the side group (vinyl and phenyl) and the noncrosslinked big chain end (free end) among polymer chains. The free end can move freely and lead to large hysteresis, which is the key factor contributing to poor rolling resistance and heat accumulation[6]; on the contrary, the vinyl group has little effect on rolling resistance whereas obvious effect on wet grip performance.[7] And the phenyl group has a middle effect between the free end and the vinyl group. According to the macromolecule design theory, the amount of free ends could be controlled by designing coupling structures or increasing polymer's number-average molecular weight ($\overline{M}_n$)[8,9]; the phenyl content could be designed by adjusting the monomer composition; and the vinyl content could be controlled by using different types and dosages of structure modifier. By far, a large number of rubber materials with novel structure, which was prepared by macromolecule design, have been reported, e.g., linear IR-SBR.[10]

In this work, a tin-coupled star-shaped block copolymer of styrene and butadiene ((SB-B)$_4$Sn) was synthesized in the way of ''core-first.''[11] A novel multifunctional organo-lithium, which contains Sn—Carbon

Correspondence to: X. Zhang (zhangxy_buct@yahoo.cn).
Contract grant sponsor: National Natural Science Foundation of China; contract grant number: 50573005.

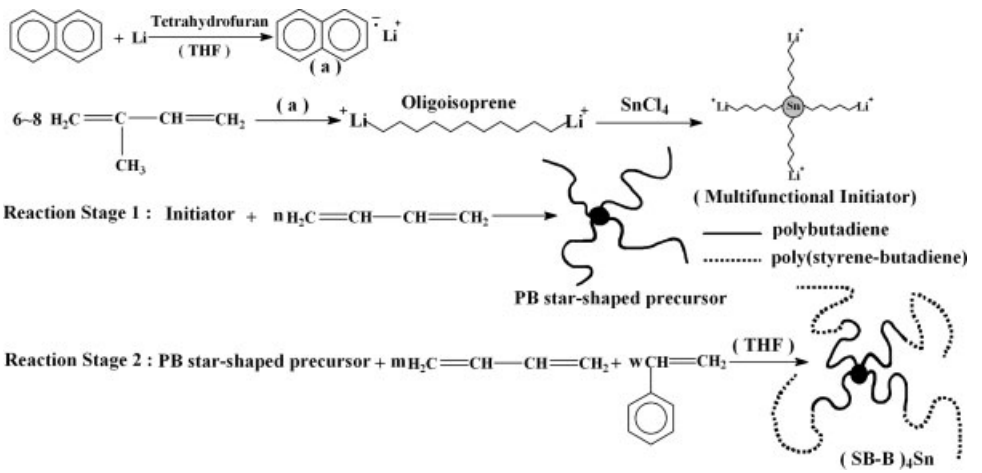

Scheme 1 Synthesis routes of $(SB\text{-}B)_4Sn$.

bonds, was used as initiator. This copolymer has a combination of high rebound blocks and large hysteresis blocks, which is expected to exhibit useful dynamic viscoelastic properties and good mechanical properties. Influence of monomer composition on the copolymer's architecture, morphology, and dynamic thermal mechanical property was investigated.

EXPERIMENTAL

Materials

The 1,3-butadiene (Bd) and isoprene (Ip) (Industrial Grade) were provided by Beijing Yansan Synthetic Rubber Factory, China. Naphthalene (analytical reagent) was purchased from Beijing chemical reagents company. Styrene (St) (Beijing Chemical Reagents Company, analytical reagent) was stirred over CaH_2 for overnight and subsequently distilled on the vacuum line, stored under nitrogen atmosphere at 0°C. Cyclohexane (Beijing Chemical Reagents Company, analytical reagent) was rectified and the cut fraction of 65–70°C was dried over Na wire under nitrogen. Tetrahydrofuran (THF) (Beijing Chemical Reagents Company, analytical reagent) was refluxed over CaH_2 for overnight and distilled under nitrogen. It was finally distilled from its sodium naphthalene solution. Alcohol (Analytical Reagent) and 2,6-di-*tert*-butyl *para*-cresol (Industrial Grade) were purchased from Beijing chemical factory. Nitrogen (≥99.999%) was provided by Beijing Shun An Qi Te Gas Company.

Synthesis

Synthetic route of star-shaped block copolymer of butadiene and styrene ($(SB\text{-}B)_4Sn$) is outlined in Scheme 1.

First, the multi-functional initiator was synthesized in two steps[12]: in the first step, the ready-made naphthalene-lithium initiated a small quantity of isoprene to form dilithiated oligoisoprene with the repeating units of 6 to 8, after 1-h reaction at 50°C in benzene solution; in the second step, coupler $SnCl_4$ was added and the reaction continued for one more hour at 50°C.

Second, a 2-L stainless steel reactor was purged with nitrogen, and subsequently washed with a living polystyryl-lithium solution. The synthesis was carried out in a two-stage procedure. The first stage was aimed to produce PB star-shaped precursor. Butadiene-cyclohexane solution and the multifunctional initiator were loaded into the reactor and the polymerization was performed at 50°C and 0.04 MPa pressure for 3 h. Subsequently in the second stage, a mixture of styrene (St), 1,3-butadiene (Bd), and THF in various compositions was added into the system and continued the polymerization at 50°C for another 3 h leading to polystyrene blocks (PS-block) or poly (butadiene-*ran*-styrene) blocks (PSB-block). Finally, the reaction was terminated using alcohol and 2,6-di-*tert*-butyl *para*-cresol. All reactions were conducted in nitrogen atmosphere.

Characterization

Average molecular weight ($\overline{M}_n$) of the multifunctional initiator was determined by Knauer 1.00 membrane permeameter at 37°C, with toluene as solvent.

Microstructures of the star-shaped block copolymer were determined by nuclear magnetic resonance instrument (NMR, Bruker AV600 MHz NMR), using $CDCl_3$ as the solvent and tetramethylsilane (TMS) as the reference.

Polydispersity index ($\overline{M}_w/\overline{M}_n$) and $\overline{M}_n$ of the star-shaped block copolymer were measured using gel permeation chromatography (GPC) (Waters150-C,

TABLE I
Formulation for Vulcanization Systems

Composition	Contents (Phr)[a]
Rubber	100
Sulfur	1.8
Zinc oxide	4.0
Carbon black	50.0
Accelerator (CZ/TT)[b]	1.0/0.2
Stearic acid	2.0
Antiager (RD)[c]	1.5
Liquid coumarrone	5.0

[a] Phr is the abbreviation of weight parts per 100 weight parts rubber.
[b] CZ = *N*-cyclohexyl-2-benzothiazole sulphenamide; TT = tetramethyl thiuram disulfide.
[c] RD = polymeried 2,2,4-trimethyl-1,2-dihydroquinoline (resin).

American) with three Waters Styragel columns (pore size 10^2, 10^3, and 10^4 Å, respectively) in series calibrated by narrow polystyrene standard with molecular weight ranging from 2.2×10^3 to 5.15×10^5 g/mol. THF was used as the eluent at a flow rate of 1.0 mL/min at 40°C.

Morphologies were tested by transmission electron microscopy (TEM, Hitachi-800-1). The specimen was cast films from toluene (0.5 wt %) at room temperature. The samples on copper grids were stained in OsO_4 vapor for 40 min. The TEM instrument worked at an accelerating voltage of 200 kV.

Processing conditions and property measurement

Samples of the star-copolymers were mixed with the additives in conventional cycles on a laboratory two-roll mill, according to the formulation given in Table I. The compounds were cured in a standard mold with about 15 MPa pressure at 150°C.

Physical mechanical properties of the star-shaped block copolymer were measured according to the ASTM standard (e.g., ASTM D2240 for shore A hardness, ASTM D412 for tensile properties, and ASTM D624 for tear strength). For each compound, five specimens were tested, and the median of the values were reported.

Dynamic mechanical properties were measured by dynamic mechanical thermal analyzer (DMTA, DDV-11-EA, Rheometric Scientific™). The experiments were carried out in the tensile mode at a heating rate of 5°C/min, a frequency of 1 Hz, and a deformation amplitude of 0.005%.

RESULTS AND DISCUSSION

Multifunctional initiator analysis

In the intermolecular coupling reaction (Scheme 1), the feeding method and dosage of $SnCl_4$ have a direct effect on functionality of the multifunctional initiator. Coupling products may exist in different forms, as is shown in Scheme 2.

These coupling products possess 2, 4, or 6 functionalities respectively, and they may exist in the initiator system simultaneously. So the functionality measured in this article is actually the average functionality (AF) of the multifunctional initiator. When the molar ratio of active lithium (Li^+) of dilithiated oligoisoprene to Cl^- in coupling agent $SnCl_4$ ($[Li^+]/[Cl^-]$) is 2, theoretical value of AF is 4 and multifunctional initiators mainly exist in the form of III. When $[Li^+]/[Cl^-]$ is larger than 2, Li^+ is excessive, some dilithiated oligoisoprene can not be coupled, thus multifunctional initiators mainly exist in the form of I and III. When $[Li^+]/[Cl]$ is less than 2, dilithiated oligoisoprene may be coupled excessively, and the form of IV and V increase. Besides, controlling the feeding speed of $SnCl_4$ can make the functionality distribution of the multifunctional initiator more uniform.

In this article, the average functionality (AF) was used to indicate the actual functionality of multifunctional initiator. AF could be calculated by the following equation:

$$\mathrm{AF} = \frac{N_2(V_N + V_I + V_s)}{W_m/\overline{M}_n}$$

where N_2 is the molar concentration of multifunctional initiator; V_N, V_I, V_S are the volume of naphthalene-lithium, isoprene and $SnCl_4$, respectively; W_m is the mass of isoprene monomer; $\overline{M}_n$ is the determined number-average molecule weight of multifunctional initiator.

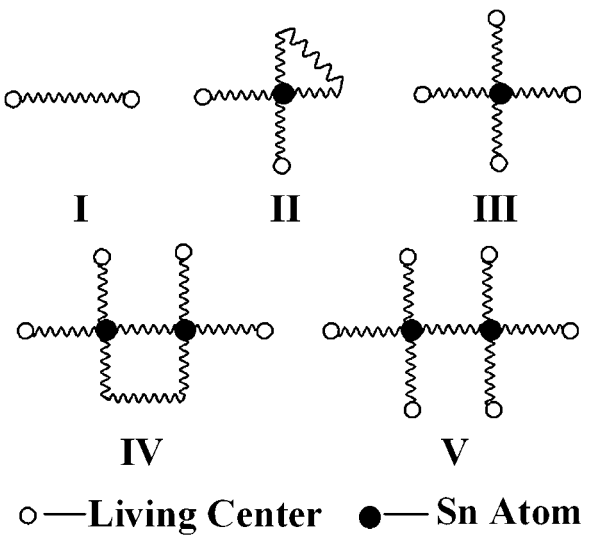

Scheme 2 Five possible coupling forms of multifunctional initiator.

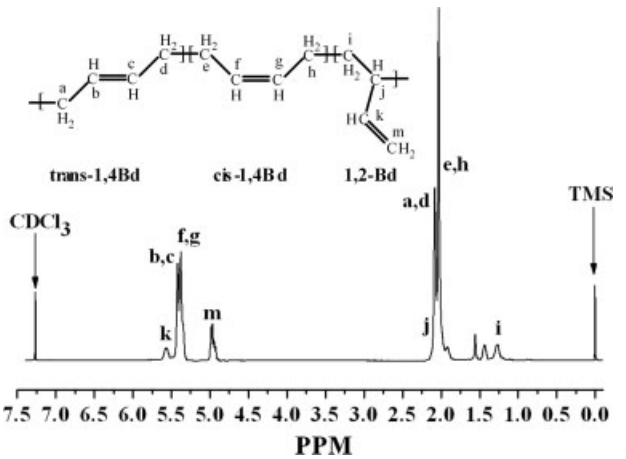

Figure 1 Microstructure and ^{1}H NMR spectrum of PB star-shaped precursor in $CDCl_3$.

Coupling degree (CD) was used to indicate the extent of coupling reaction, and could be calculated according to the following equation:

$$\mathrm{CD} = \frac{N_1(V_N + V_I) - N_2(V_N + V_I + V_S)}{4N_S V_S} \times 100\%$$

where N_1, N_S are the molar concentration of dilithiated oligoisoprene and $SnCl_4$, respectively.

For preparing the multifunctional initiator with four functionalities, $[Li^+]/[Cl^-]$ was designed to be two in this article. For ensuring that Cl^- in $SnCl_4$ react entirely with Li^+ of dilithiated oligoisoprene, during the coupling reaction, $SnCl_4$ was added drop by drop and the reactant was stirred quickly. As a result, AF of the multifunctional initiator is 3.95, close to the theoretical value. And CD value is 99% which implies that Cl^- and Li^+ reacted entirely during the coupling reaction.

^{1}H NMR results analysis

Figure 1 illustrates the ^{1}H NMR spectrum of the PB star-shaped precursor sampled at the end of first reaction stage. Figure 2 shows the ^{1}H NMR spectrum of $(SB\text{-}B)_4Sn$.

In Figure 1, sharp signals for paraffinic methylene protons of *cis*-1,4-butadiene units (e, h) and *trans*-1,4-butadiene units (a, d) are observed at 1.98–2.04 ppm and 2.06–2.11 ppm, respectively. The peak at 1.26–1.30 ppm represents paraffinic methylene protons of vinyl structures (i). The peaks at 4.79–4.99 ppm and 5.55–5.59 ppm represent protons of $=CH_2$ (m) and $-CH=$ (k) of vinyl structures, respectively. The peak at 5.37–5.40 ppm displays protons of $-CH=$ of *cis*-1,4-butadiene (f, g). The peak of $-CH=$ of *trans*-1,4-butadiene (b, c) appears at 5.41–5.45 ppm.[13–15]

Vinyl content based upon the amount of 1,3-butadiene in PB star-shaped precursor can be calculated according to the following equation[16]:

$$(\mathrm{Bv/PB})\% = \frac{2I_{(4.79-4.99)}}{I_{(4.79-4.99)} + 2I_{(5.37-5.60)}} \times 100\%$$

where (Bv/PB)% means the vinyl content (Bv%) in PB star-shaped precursor; I indicates the peak area of proton at the chemical shift area indicated in the bracket.

In the first stage, polymerization of 1,3-butadiene monomers was initiated by the multifunctional organolithium initiator. The initiator system had a ratio of THF to organolithium around 0.8, which led to low vinyl content within PB star-shaped precursor. ^{1}H NMR results show that PB star-shaped precursors of all samples possess similar microstructures. Their vinyl contents (Bv%) are in the range of 18.0–21.0%, and the *cis*-1,4-structure is predominant.

In the second stage, 1,3-butadiene and styrene monomers with different compositions were reacted in the presence of regular modifier THF. A ratio of 60/1, THF/organolithium ([THF]/[Li]), was used for all the second reaction stages. Microstructure of PSB-blocks was not only influenced by THF, but also affected by the monomer composition. Microstructure data can be calculated from Figure 2. The proton signal peak of styrene units is appeared at 6.20–7.40 ppm; and the signal peak of 1,3-butadiene units is appeared at 4.80–5.60 ppm. The difference within the 1,3-butadiene signal peaks between Figures 2 and 1 is that vinyl signal peak area in Figure 2 is much bigger than that in Figure 1.

Figure 3 illustrates the vinyl content based upon the amount of 1,3-butadiene within PSB-blocks as a function of styrene content in loading solution (St%).

For the homopolymerization of 1,3-butadiene in presence of THF, the vinyl content in homo-polybutadiene increases as the ratio of THF to reactive lithium ([THF]/[Li]) increases. When the ratio increases

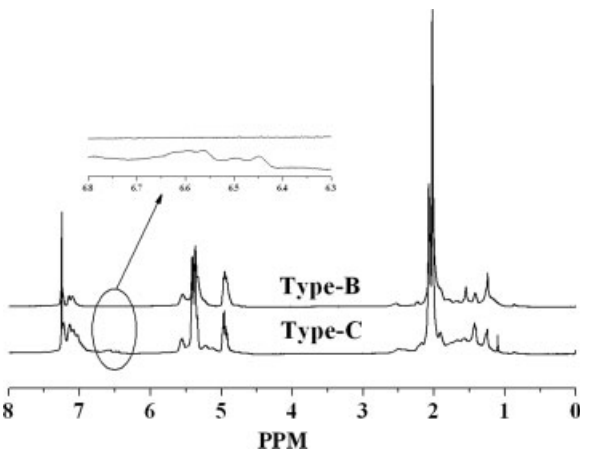

Figure 2 ^{1}H NMR spectrum of $(SB\text{-}B)_4Sn$ in $CDCl_3$.

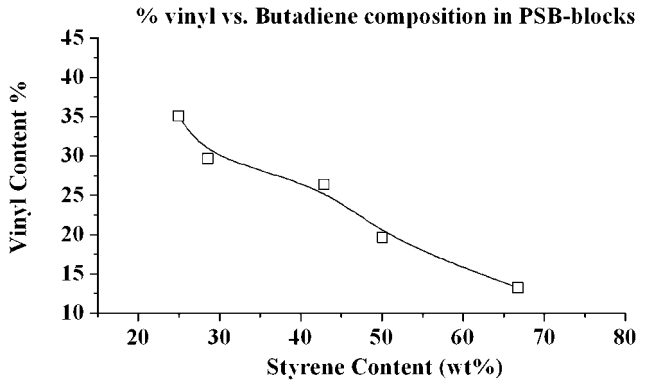

Figure 3 Vinyl content within PSB-blocks as a function of styrene composition.

to 60, the vinyl content will reach to 50–60%.[17,18] In the second reactive stage, the ratio of [THF]/[Li] is 60. Figure 3 shows that vinyl contents based upon the 1,3-butadiene composition within PSB-blocks are lower than 35.0%. Furthermore, Figure 3 gives a linear curve that decreases as the amount of styrene is increased. As the styrene content rises from 25.0 to 66.8%, the vinyl content decreases from 35.0 to 13.2%. It means that the influence of THF on the microstructure is limited as the styrene content is increased.

Figure 2 also shows that two different ^{1}H NMR spectra (type-B and type-C) are observed in the star-shaped block copolymer $(SB\text{-}B)_4Sn$. Their difference exists in the signal peak of homo-polystyrene appearing at 6.20–6.85 ppm.

It is well known that homo-polystyrene exhibits double peaks in ^{1}H NMR spectrum, which are located at 6.20–6.85 ppm and 6.85–7.40 ppm, respectively.[19] The area ratio of the former to latter is 2/3, and the peak at 6.20–6.85 ppm is smaller. Styrene units which are randomly distributed only show one single peak at 6.85–7.40 ppm. If copolymer contain both homo-polystyrene blocks and random styrene units, the area ratio of 6.20–6.85 ppm to 6.85–7.40 ppm will be lower than 2/3.

In ^{1}H NMR spectrum of type-B (Fig. 2), there is no signal peak at 6.20–6.85 ppm. This result illustrates that styrene units are distributed randomly in type-B. So type-B possesses a diblock structure: the polybutadiene block (PB-block) and the poly(butadiene-*ran*-styrene) block (PSB-block). On the contrary, ^{1}H NMR spectrum of type-C contains signal peaks at 6.20–6.85 ppm, and the area ratio of 6.20–6.85 to 6.85–7.40 ppm is smaller than 2/3. We could conclude that homo-polystyrene blocks (PS-block) appear in type-C. Thus type-C contains a triblock structure: PB-block, PSB-block and PS-block.

The PS-block content can be calculated according to the following equations, and the calculated results are illustrated in Figure 4.

$$(T-St)\% = \frac{I_{(6.20-6.85)} + I_{(6.85-7.40)}}{I_{(6.20-6.85)} + I_{(6.85-7.40)} + 0.649 \times \left[I_{(4.79-4.99)} + 2 \times I_{(5.37-5.60)}\right]} \times 100\%$$

$$(\mathrm{PS-block})\% = \frac{2.5 \times I_{(6.20-6.85)}}{I_{(6.20-6.85)} + I_{(6.85-7.40)}} \times St\%$$

where (*T*-*St*)% means the total styrene content in the copolymer $(SB\text{-}B)_4Sn$, and (PS-block)% means the weight percent of homo-polystyrene based upon the total composition of $(SB\text{-}B)_4Sn$.

Figure 4 illustrates the relationship between the (PS-block)% and the styrene content in loading solution (St%). In Figure 4, the curve shows a turning point at a composition of 34.9% styrene in the loading solution. When the St% is less than 34.9%, the PS-block can not be detected, and the styrene units are randomly arranged in the copolymer chain. When the St% reaches 42.9%, the PS-block is generated and its weight content is 4.2%. Further increasing the styrene content, PS-block contents increase to higher level. This indicates that THF fails to randomize styrene-butadiene copolymer when the styrene content is higher than 42.9%. In other words, the regulation effect of THF is limited to low styrene contents ($\leq$34.9%). Above that content, styrene units no longer randomly distribute, but form homogeneous blocks.

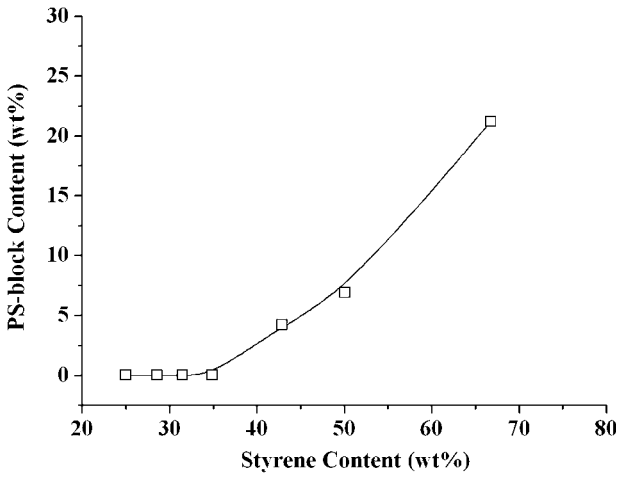

Figure 4 The PS-block content versus styrene content in loading solution.

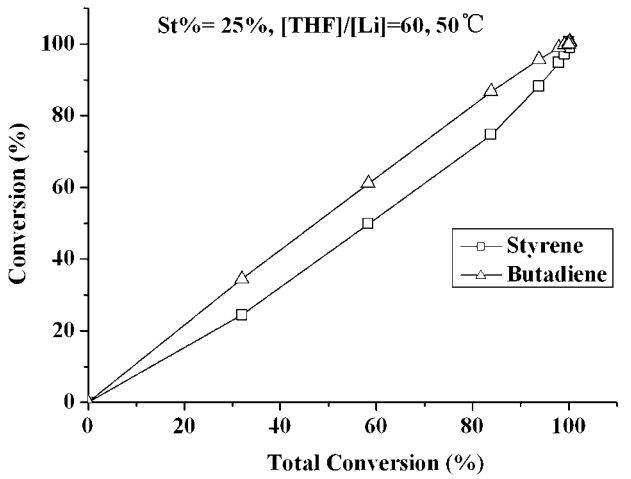

Figure 5 Monomer conversion versus total conversion for the PSB-block.

Copolymerization kinetics analysis

Figure 5 illustrates the individual monomer conversion as a function of the total monomer conversion in the second polymerization stage. The graphs show that 1,3-butadiene monomers and styrene monomers are consumed at different rates. The large discrepancy between two curves implies that 1,3-butadiene has a larger reactivity ratio than styrene in the present reactive conditions. Accordingly, 1,3-butadiene monomers were incorporated into the copolymer chains faster than styrene monomers. Figure 6 shows the relationship between copolymer composition and the total conversion. With the consumption of the monomers, the 1,3-butadiene content in the copolymer decreases while the styrene content increases. Thus, the distribution of the styrene unit in the copolymer chain exhibits a concentration gradient: poor in one side and becoming rich toward the other side. If the styrene content in the loading solution is sufficiently high, after the 1,3-butadiene is substantially used up, homo-blocks of polystyrene will be formed at the chain end. This implies that PS-blocks in type-C are formed at the copolymer chain end. The copolymerization kinetics helps to confirm the sequence of different blocks incorporated into the star-shaped block copolymer $(SB\text{-}B)_4Sn$. The four functionality architectures of type-B and type-C are described in Scheme 3.

Scheme 3 shows that the molecular architecture of type-B is star-shaped polybutadiene-*b*-poly(butadiene-*ran*-styrene) (*S*-PB-PSB); and that of type-C is star-shaped polybutadiene-*b*-poly(butadiene-*ran*-styrene)-*b*-polystyrene (*S*-PB-PSB-PS). So we could conclude that $(SB\text{-}B)_4Sn$ possesses two different types: *S*-PB-PSB and *S*-PB-PSB-PS.

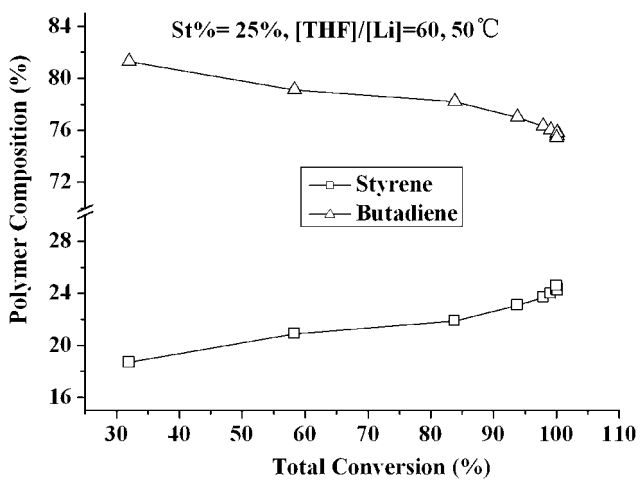

Figure 6 Polymer composition versus total conversion for the PSB-block.

GPC results analysis

GPC results show that both PB star-shaped precursor and star-shaped block copolymer $(SB\text{-}B)_4Sn$ have wide polydispersity. The polydispersity index of PB star-shaped precursor ranges from 1.7 to 2.2; and that of $(SB\text{-}B)_4Sn$ ranges from 1.5 to 1.8.

The wide polydispersity is mainly caused by the characteristics of multifunctional initiator. The multifunctional initiator, as aforementioned, is composed of different molecular forms which possess different functionalities. Copolymers prepared by this initiator will also contain different functionalities, thus, their polydispersity is widened.

At the first reactive stage, the polymer chain has a small length, which leads to little enwrapping effect on the initiated ability of the initiator. Thus all the active centers have the similar reactive speed. As a result, influence of the functionality on the polydispersity become obvious and the PB star-shaped precursor displays a wide polydispersity index ranging from 1.7 to 2.2. At the second reactive stage, the big

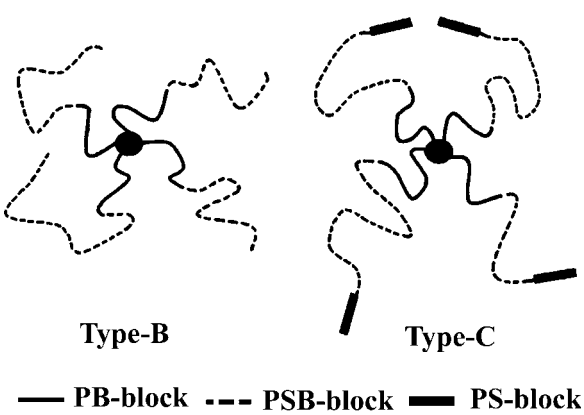

Scheme 3 Sketch maps of two different types of $(SB\text{-}B)_4Sn$.

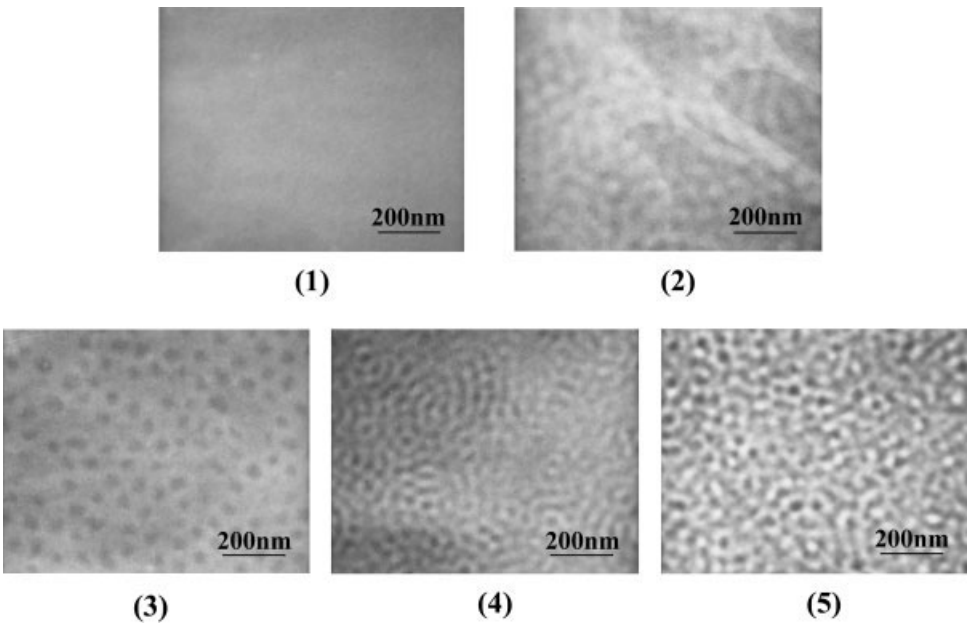

Figure 7 TEM images of $(SB\text{-}B)_4Sn$ (stained with OsO_4 for 40 min).

length of polymer chains leads to a sever entanglement, and the reactive speed is slowed down because living centers are enwrapped by molecular chains. Copolymer molecules with larger number of functionality exhibit more sever entanglement effect, thus their reactive speed are slower than other molecules. As a result, all of the copolymer chain length has the tendency to become uniform and the polydispersity index is decreased to the range of 1.5–1.8.

This wide polydispersity is beneficial to the star-shaped block copolymers, because wide polydispersity could help to improve copolymer's processing properties.[20]

Morphology analysis

TEM images of five different samples of $(SB\text{-}B)_4Sn$ are illustrated in Figure 7, and their microstructure data are summarized in Table II.

Figure 7 displays TEM images of **sample 1** to **sample 5**. For **sample 1**, there are two types of blocks: homogenous PB-blocks and butadiene-*ran*-styrene ones. It is indicated in Table II that the copolymer block (PSB-block) possesses a low styrene content (25 wt %) and thus compatible with homo-PB ones. As a result, the morphology exhibits a single phase. **Sample 2** contains the same type of blocks as **sample 1**, however, the styrene content is a little higher (28.6 wt %). Such a small increment in styrene content is, however, sufficient to decrease the compatibility with homo-PB blocks, resulting in minor phase separation. One may notice the PB domains (black) are separated by copolymer ones (gray).

As the styrene content in the loading solution is increased, homo-PS blocks will be formed, e.g., in **sample 3**. Since that the copolymer block possesses a higher styrene content, it becomes compatible with homo-PS blocks and more incompatible with homo-PB blocks. As a result of phase separation, homo-PB blocks form islands in a sea of copolymer and homo-PS blocks.

At higher styrene content in the loading solution, two consequences could happen: (i) the styrene content in the copolymer became comparable with that

TABLE II
Weight Percent of Each Blocks Based Upon the Total Weight of $(SB\text{-}B)_4Sn$

Sample No.	$\overline{M}_n \times 10^{-4}$	$\overline{M}_w/\overline{M}_n$	PB-block (wt %)	PSB-block		PS-block (wt %)
				Styrene/PSB (wt %)	Vinyl/PSB (wt %)	
1	16.9	1.7	40.3	25.0	26.3	0
2	34.0	1.8	23.0	28.6	21.1	0
3	17.0	1.5	26.1	39.5	15.9	4.2
4	19.6	1.8	41.5	43.4	11.1	6.9
5	23.3	1.8	31.9	51.8	5.1	21.2

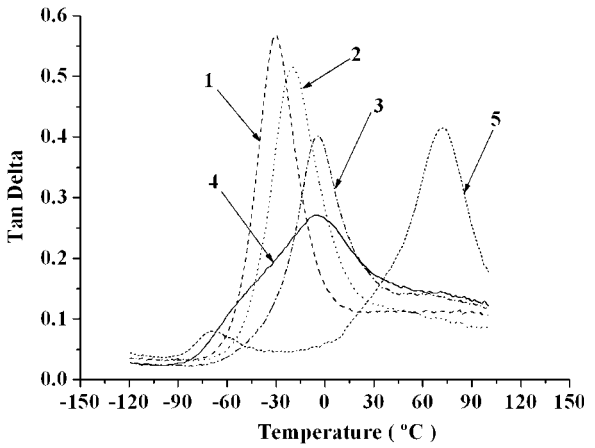

Figure 8 DMTA (tan δ) spectra of $(SB\text{-}B)_4Sn$.

of butadiene, (ii) larger fractions of homo-PB and PS-blocks were generated. As in **sample 4**, the system is composed of two phases, the homo-PB block is one, and the copolymer and homo-PS constitute another. Since the content of homo-PB blocks is also high, the morphology is no longer sea-island, but bi-continuous. However, one may detect the degree of phase separation from the color of the micrographs: for **sample 4**, the black PB domain is mingled with gray area; but for **sample 5**, the black PB domain is penetrated in almost white media, because of the different styrene contents.

Dynamic property analysis

Figure 8 presents the DMTA spectra of different star-block copolymers. **Samples 1**, **sample 2**, and **sample 3** each display a single loss peak. However, the reasons are different. **Sample 1** is a homogeneous system; one loss peak is the natural result. For **sample 2**, although minor phase separation occurred, which was not seriously enough to produce a second loss peak, a single loss peak is observed. However, because of the higher styrene content, the peak is shifted to a higher temperature and is somewhat broadened. The same mechanism could be partially applied to the **sample 3**. As shown in Figure 7, this sample forms a sea-island morphology. First, the size of PB domain is small, its movement is not sufficient to contribute a detectable loss peak. More importantly, if the system has been composed by two individual polymers, a second loss peak for homo-PB would have been observed. However, in a block copolymer, the movement of PB-blocks is partially inhibited by adjacent blocks. Consequently, only one loss peak is exhibited, which, as explained in above section, is contributed by homogeneous blend of copolymer and PS-blocks.

Sample 4 gives rise to a broad loss peak, covers a wide temperature range, from −70 to 30°C. As aforementioned, **sample 4** possesses a morphology of two continuous phases: one is homo-PB, and the other is the composed one of the copolymer and homo-PS blocks, which should have contributed a loss peak each. However, since the content of homo-PS blocks is low (6.9 wt %), and the copolymer blocks may act somewhat as a compatibilizer between PB-blocks and PS-blocks, for this reason, the two loss peaks shift towards each other, resulting in a broadened peak.

In **sample 5**, the fraction of homo-PS blocks is high. Its mixing with the copolymer blocks causes the latter to become quite incompatible with the homo-PB block; as a result, serious phase separation occurs. Indeed, Figure 8 shows two loss peaks far apart from each other. The low peak at −70°C for homo-PB blocks and the other one at 73°C for the composed phase of copolymer and homo-PS blocks. Compared with the morphologies in Figure 7, one could recognize that although **sample 4** and **sample 5** show similar bi-continuous phases, different only in color, they are in quite different status of degree of phase separation.

Mechanical property analysis

Mechanical properties of five different kinds of rubber are summarized in Table III. The tensile strength

TABLE III
Mechanical Properties of Five Different Kinds of Rubbers

	$(SB\text{-}B)_4Sn$	IR-SBR[10]	SBR-IR-SBR[5]	SSBR[21] (Tufdene)	E-SBR[22] (SBR-1500)
St%	31.6	–	29.6	–	23.5
Bv%	23.5	–	39.6	–	–
Shore A hardness	74	–	82	59	65
Tensile strength (MPa)	20.2	26.0	17.0	18.7	25.4
Elongation at break (%)	445	–	371	519	548
Modulus at 300% elongation (MPa)	12.2	10.0	13.1	8.8	10.6
Permanent set (%)	16	–	10	8	–
Tear strength (KN/M)	41.4	–	33.0	30.0	47.0
Loss factory (tan δ)					
0°C	0.38	0.31	0.20	0.35	0.17
60°C	0.14	0.13	0.14	0.13	0.15

of the star-shaped copolymers prepared in this study is around 20 MPa lower than that of IR-SBR (26.0 MPa) and E-SBR (25.4 MPa), but higher than that of SBR-IR-SBR and SSBR. Modulus at 300% elongation and tear strength of $(SB\text{-}B)_4Sn$ are better than that of other rubbers. According to Satio,[23] the value of tan δ at 0°C indicates the wet skid resistance of rubbers. In Table III, tan δ value of $(SB\text{-}B)_4Sn$ at 0°C is 0.38, higher than that of the others. It means the wet skid resistance of $(SB\text{-}B)_4Sn$ is much better than that of other rubbers. Tan δ value at 60°C indicates the rolling resistance, and lower tan δ value implies lower rolling resistance.[23] Tan δ value of $(SB\text{-}B)_4Sn$ at 60°C is 0.14, similar to the value of other rubbers. Table III shows that $(SB\text{-}B)_4Sn$ has the similar mechanical properties and rolling resistance property with ESBR, SSBR (Tufdene), and IR-SBR, but its wet skid resistance property is much better than that of the others. So we could conclude that $(SB\text{-}B)_4Sn$ can satisfy the performance requirements of high performance tire tread.

CONCLUSIONS

In the two-stage polymerization of star-shaped block copolymers, homo-polybutadiene block was first formed, and the composition of the subsequent block was determined by the styrene content in the loading solution at the second reaction stage. When the styrene content was lower than 34.9%, poly(butadiene-*ran*-styrene) block was generated, leading to a star-shaped diblock copolymer. If the styrene content reached 42.9%, after the butadiene units were substantially consumed, homo-polystyrene blocks were formed at the end of the chains, resulting in a star-shaped triblock copolymer. The styrene content also had a significant influence on the microstructures of butadiene units in the poly(butadiene-*ran*-styrene) blocks. With increasing styrene content from 25.0 to 66.8%, the content of vinyl structure decreased from 35.0 to 13.2%. Depending on the architectures, sea-island or bi-continuous morphologies of the copolymers were exhibited, and various dynamic mechanical properties were displayed. Mechanical tests showed that mechanical properties of $(SB\text{-}B)_4Sn$ are similar to that of ESBR, SSBR (Tufdene), and other rubber materials. Moreover, $(SB\text{-}B)_4Sn$ has a good overall balance property of high wet skid resistance and low rolling resistance properties, and could be used to produce high performance tire tread.

References

1. Chen, S. C. China Synth Rubber Ind 1995, 18, 260.
2. Chang, Y.; Chen, S. C.; Cao, Z. G. China Elastomerics 1994, 4, 35.
3. Tsutsumi, F.; Sakakibara, M.; Oshima, N. Rubber Chem Technol 1990, 63, 8.
4. Paul, D. R.; Newman, S. Polymer Blends; Academic Press: New York, 1978; Vol. 2.
5. Xu, H. D.; Xu A. L.; Zhang, X. Q.; Guan, Y. Y.; Xiu, X. H.; Li, Y. China Elastomerics 2003, 13, 34.
6. Takao, H.; Imai, A. China Synth Rubber Ind 1987, 1 (Suppl), 33.
7. Wilder, C. R.; Haws, J. R. Kautsch Gummi Kunstst 1984, 37, 2885.
8. Ohshima, N.; Tsutsumi, F.; Sakakibara, M. China Synth Rubber Ind 1987, 1 (Suppl), 35.
9. Kern, W. J.; Futamura, S. Polymer 1988, 29, 1801.
10. Hsu, W. L.; Halasa, A. F. US Patent US 5,070,148 (1991).
11. Ishizu, K.; Uchida, S. Prog Polym Sci 1999, 24, 1439.
12. Zhang, X. Y.; Jin, G. T.; Zhao, S. H. US Patent, US 6,150,487 (2000).
13. Wang, S.; Luo, X. L.; Ma, D. Z.; Huang, Y. P. Chin J Chem Phys 2004, 17, 652.
14. Dutta, N. K.; Choudhury, N. R.; Haidar, B.; Vidal, A. Rubber Chem Technol 2001, 74, 260.
15. Huang, Y. P.; Chen, G. M.; Wang, S.; Li, H. W.; Ma, D. Z. Chin J Appl Chem 2005, 22, 431.
16. Wu, G. F.; Wang, S. C.; Zhang, L. China Chem Technol 1982, 3, 44.
17. Jin, G. T. Advance in Theory and Appliance of Polymer Chemistry; Petrochemical Industry Press: Beijing, 1995.
18. Jin, G. T.; Fan, L. Q.; Xu, R. Q. J Beijing Inst Chem Technol 1988, 15, 6.
19. Mochel, V. D. Rubber Chem Technol 1967, 40, 1200.
20. Gong, H. Y.; Zhang, S. Z.; Liu, R. Q.; Fang, Z. M. China Synth Rubber Ind 1987, 10, 428.
21. Ji, F. C.; Li, W.; Wang, X.; Liu, T. H.; Liang, A. M. China Elastomerics 2003, 13, 9.
22. Zhao, S.; Zhang, X.; Jin, G. J Appl Polym Sci 2003, 89, 2311.
23. Satio, K. Y. Kautsch Gummi Kunstst 1986, 39, 30.